Advances in Engineering Research : Possibilities and Challenges
ISSN Print: 3079-5192
ISSN Online: 3079-5206
https://doi.org/10.63313/AERpc.9094

Research on Surface Deformation Monitoring and Stability of Mined-out Areas Based on SBAS InSAR Technology

Yuhao Zhang
School of Energy Science and Engineering, Henan Polytechnic University, Jiaozuo 454000, China
Email: 306855932@qq.com

How to cite this paper: Zhang, Y. H. (2026). Research on surface deformation monitoring and stability of mined-out areas based on SBAS InSAR technology. Advances in Engineering Research: Possibilities and Challenges, 4(1), 135–143. ISSN (Print): 3079-5192; ISSN (Online): 3079-5206.
https://doi.org/10.63313/AERpc.9094
Published: 2026-04-30

Copyright © 2026 by author(s) and Erytis Publishing Limited.
This work is licensed under the Creative Commons Attribution International License (CC BY 4.0).
http://creativecommons.org/licenses/by/4.0/



Abstract

Long-term surface deformation over old mined-out areas overlain by thick unconsolidated strata in North China is prominent. Traditional monitoring approaches are difficult to achieve large scale, long time series, and high precision dynamic observations. To scientifically understand the spatiotemporal evolution of surface subsidence and site stability characteristics of old mined out areas, this paper takes the mined out areas of Panels 2301, 2302, and 2303 in the No.5 Coal Mine of Hebi Mining Group, Shancheng District, Hebi, Henan Province as the study object. Using the SBAS InSAR time series interferometric technique, 110 scenes of Sentinel 1A images from November 2015 to December 2024, combined with 30 m resolution SRTM DEM data and ESA precise orbit data, are adopted to invert the spatiotemporal distribution of annual average surface deformation rate and cumulative deformation over the past decade. Through time series subsidence curve analysis of typical monitoring points, profile comparison, and accuracy verification, the staged evolution and spatial differentiation of surface subsidence above goafs under thick unconsolidated strata are revealed. The results show that the study area is dominated by surface subsidence, with a maximum subsidence rate of −36 mm/a and an average rate of 2.35 mm/a. The spatial pattern of subsidence exhibits an obvious funnel shaped stepwise decrease. Around 2018, surface subsidence in the study area generally shifted from the rapid development stage to the residual deformation stage with slow attenuation. The attenuation rate shows significant spatial differences controlled by fault locations, panel conditions, and geological structures. Panel 2303, with a later stopping time, shows the most active subsidence, while Panels 2301 and 2302, mined earlier, have become basically stable. The SBAS InSAR results agree well with leveling measurements, and the monitoring accuracy meets the requirements for goaf stability evaluation. The findings can provide reliable technical support and scientific basis for land redevelopment, construction site selection, geological hazard risk assessment, and long term safety monitoring of old mined out areas in the Hebi mining area

Keywords

SBAS Insar; Old Mined Out Area; Surface Subsidence; Time Series Evolution; Thick

Unconsolidated Strata; Mining Area Stability

1. Introduction

Surface subsidence induced by coal mining is a common geo-environmental problem in mining areas. Under thick unconsolidated overburden conditions, surface deformation is characterized by long duration, significant residual subsidence, and complex spatial distribution, which poses long-term risks to engineering structures and land utilization. Therefore, investigating the spatiotemporal evolution of surface subsidence is of great importance for mining safety assessment and land reclamation.

Traditional monitoring methods, such as leveling surveys and Global Navigation Satellite Systems (GNSS), provide high accuracy but are limited by sparse spatial coverage, high cost, and difficulty in achieving continuous large-scale monitoring. Interferometric Synthetic Aperture Radar (InSAR) has become an important tool for surface deformation monitoring due to its wide-area coverage, high precision, and all-weather observation capability [1]. However, Differential InSAR (D-InSAR) is susceptible to temporal decorrelation and atmospheric delays in long-term deformation analysis, which limits its applicability [2]. To overcome these limitations, Persistent Scatterer InSAR (PS-InSAR) and Small Baseline Subset InSAR (SBAS-InSAR) techniques have been developed. Among them, SBAS-InSAR improves the stability of time-series deformation retrieval by constructing a network of interferograms with small temporal and spatial baselines [3–5], and has been widely applied in mining subsidence monitoring [6–8].

Therefore, this study utilizes Sentinel-1A SAR data from 2015 to 2024 and applies the SBAS-InSAR technique to retrieve time-series surface deformation in the study area. The objectives are to analyze the spatiotemporal evolution of subsidence, investigate the influence of fault structures, and validate the monitoring accuracy using leveling measurements..

2. Engineering Overview and Construction Technology

2.1. Working Face Overview

The study area is located in the No.5 Coal Mine of Hebi Mining Group, Shancheng District, Hebi City, Henan Province, in the transitional zone between the North China Plain and the Taihang Mountains. The terrain dips gently from northwest to southeast with small topographic relief. Tang River and other seasonal watercourses cross the mine from northwest to southeast. Long term intensive coal mining has formed numerous subsidence basins and continuous deformation zones, significantly affecting the ecological environment, land use, and residential safety.

This study focuses on Panel 2303, located in the south wing of the third section, with strike length ~450 m, dip length 100 m, average mining depth 391.5 m, and seam

thickness 8.94 m. It was mined out in July 2015 and is a typical thick seam, medium depth, nearly horizontal old goaf. The immediate roof is weak carbonaceous mudstone; the main roof is 15 m thick fine grained sandstone, forming a "soft lower, hard upper" structure favorable for long term subsidence.

Table 1. Conditions of coal seam roof and floor

Panel	Mining Period	Thickness (m)
2301	2009.2–2010.9	8
2302	2010.11–2012.10	8.9
2303	2014.3–2015.7	9

2.2. Surface Deformation Characteristics and Analysis

Field investigation shows widespread mining induced hazards: goaf collapse, ground fissures, wall cracking, uneven settlement, etc. Ground fissures and leakage are severe along the Tang River, with local collapse depths up to meters. Groundwater levels have declined significantly, increasing the risk of secondary hazards such as slope failure and reactivated subsidence.

Surface collapse is dominated by mining induced goaf collapse. After coal extraction, overburden loses support, bends, fractures, and caves, propagating to the surface. The thick unconsolidated strata lead to long duration, hysteretic, and time dependent subsidence, even years after mining cessation. With planned industrial construction and land reuse, systematic stability assessment is critical for safe development.

3. InSAR Data and Technical Principles

3.1. SAR Data and Auxiliary Data

To reveal the long-term evolution of residual surface subsidence in old goafs under thick unconsolidated strata, this study employs the Small Baseline Subset InSAR (SBAS-InSAR) technique to monitor surface deformation over the period from 2015 to 2024. A total of 110 Sentinel-1A ascending single-look complex (SLC) images acquired between November 20, 2015 and December 26, 2024 are selected for time-series inversion. These images fully cover Panels 2301, 2302, and 2303 as well as surrounding areas, satisfying the monitoring requirements for multi-panel superimposed mining conditions.

Precise Orbit Determination (POD) data from ESA are used to correct orbital parameters and reduce orbital errors. The 30 m × 30 m resolution SRTM DEM from

NASA is employed to remove flat-earth and topographic phases. The specific parameters of the Sentinel-1A images are listed in Table 2.

Table 2. Parameters of the Sentinel-1A images

Data type	IW
Polarization mode	VV
Orbit direction	Ascending
Main imaging dates	20151120、20151214、20160107、20160309、20160412、20160530、20160927、20161009、20161102、20161208、20170102、20170206、20170302、20170407、20170501、20170616、20170712、20170805、20170910、20171016、20171109、20171215、20180402、20180508、20180613、20180707、20180812、20180906、20181011、20181116、20181222、20190316、20190620、20190912、20191229、20200602、20201211、20211228、20221223、20231220、20241226

3.2. SBAS-InSAR Principle

InSAR extracts surface deformation from phase differences between two SAR images. Traditional D-InSAR suffers from temporal and spatial decorrelation in long-term monitoring. SBAS-InSAR overcomes this limitation by constructing an interferogram network with small temporal and spatial baselines.

Assuming N+1 SAR images acquired at times ‘t’, ‘t_1’,..., ‘t_n’, a set of M interferograms is formed under baseline constraints. After removing topographic, atmospheric, orbit and noise phases, the differential interferometric phase for the ‘j’-th interferogram (acquired at ‘t_a’ and ‘t_x’) can be expressed as:

$$\Delta\phi_j(x,y) = \frac{4\pi}{\lambda}[d(t_b,x,r) - d(t_a,x,\gamma)]$$

where λ is the wavelength, and ‘d’ represents the line-of-sight (LOS) displacement. For M ≥ N, the unknown displacements are solved using least squares or singular value decomposition (SVD).

The LOS displacement is converted to vertical subsidence by:

$$d_v = \frac{d_{LOs}}{\cos\theta}$$

where θ is the radar incidence angle. This conversion is valid because residual deformation in the old goaf is dominated by vertical settlement.

3.3. Data Processing Workflow

The SBAS-InSAR processing is carried out on the SARscape platform. The main steps include:Image coregistration and super-master selection: All SLC images are

coregistered to a super-master image with optimal geometric quality. Small baseline network construction: A temporal baseline threshold of 120 days and a spatial baseline threshold of 2% of the critical baseline are applied to generate interferometric pairs . Interferogram generation and topographic phase removal: Differential interferograms are generated and the topographic phase is removed using SRTM DEM . Filtering and phase unwrapping: Goldstein filter and minimum cost flow (MCF) algorithm are used. Orbital refinement and re-flattening: POD data and stable high-coherence points outside the mining-affected area are used to correct residual orbital errors. Time-series inversion: The least squares and SVD method are combined to estimate cumulative deformation and mean deformation rate. Atmospheric phase is further corrected by temporal high-pass filtering and spatial low-pass filtering. Geocoding: Results are transformed from radar coordinates to geographic coordinates. The complete processing flow is shown in Figure .

4. Results and Analysis

4.1. Spatiotemporal Evolution of Cumulative Subsidence and Fault Control

To analyze the staged evolution, cumulative subsidence maps for three periods are presented in Figure 1. Figure 2 shows the spatial relationship among panels, faults, and profile lines.

2015–2017: Subsidence first appears near the working faces with limited extent, dominated by local subsidence.2017–2018: The subsidence area expands significantly, and a subsidence basin begins to form.2018–2024: Multi-panel subsidence basins become well-developed and overlap with each other. Obvious differential subsidence occurs near the faults.

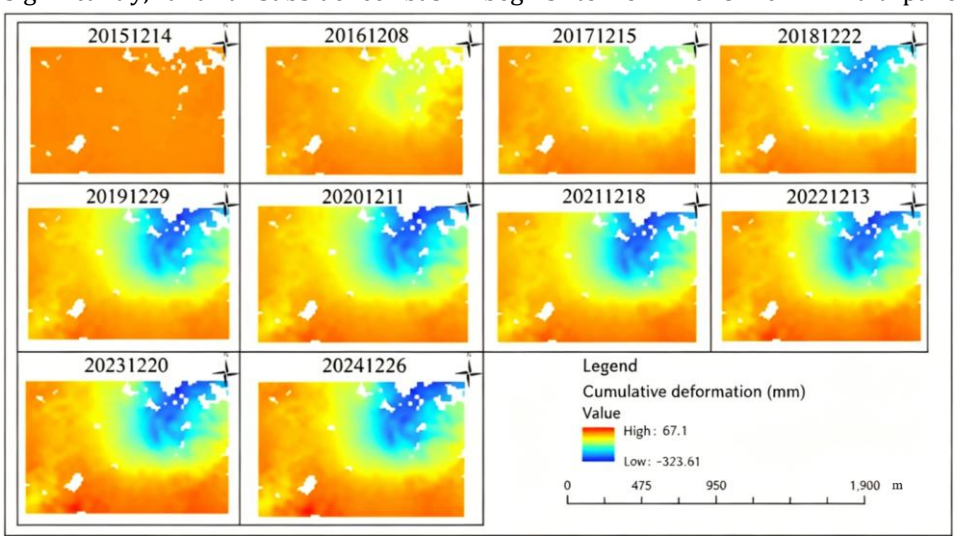


Figure 1. Time-series Cumulative Settlement Diagram

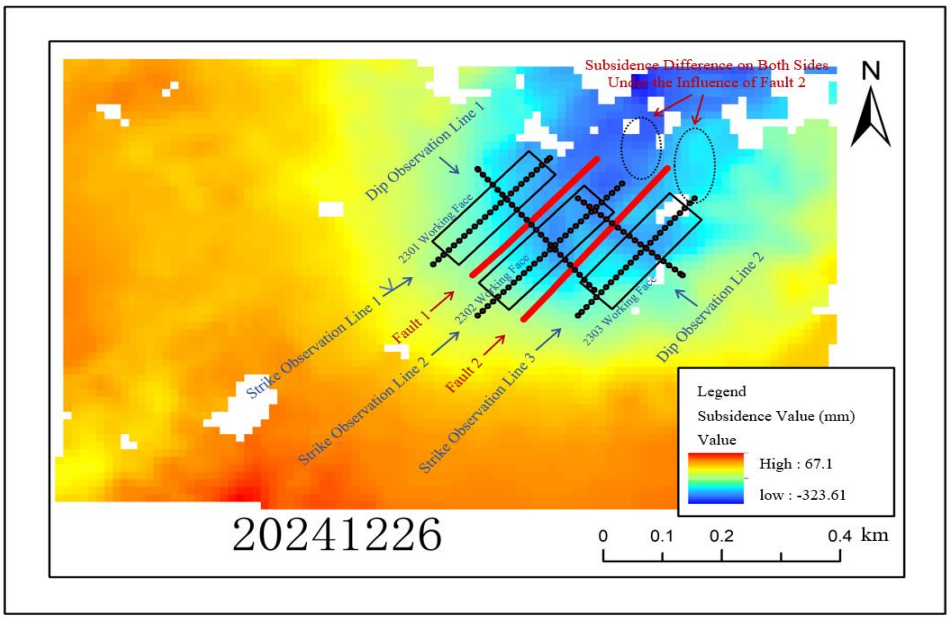
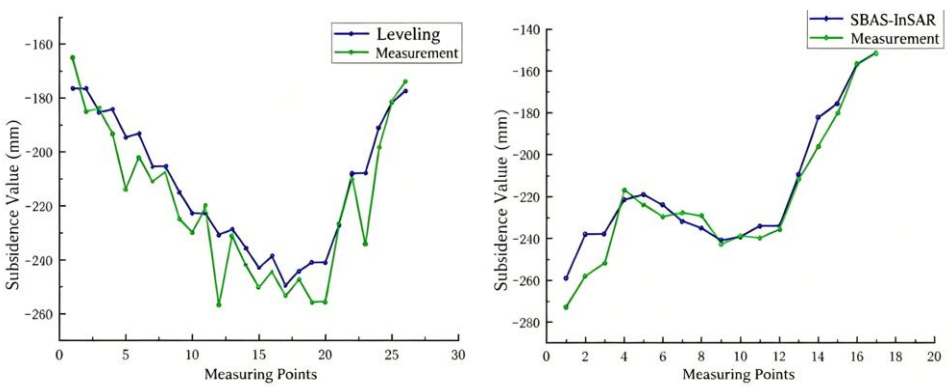


Figure 2. Spatial Relationship Diagram of Working Face, Faults and Section Lines

Fault 1 (adjacent to Panels 2301 and 2302) shows moderate spatial heterogeneity, acting as a transitional regulator. Fault 2 (between Panels 2302 and 2303) exhibits strong asymmetric subsidence with clear hanging wall/footwall differences, indicating a stronger fault control on subsidence distribution.

4.2. Accuracy Validation with Leveling Measurements

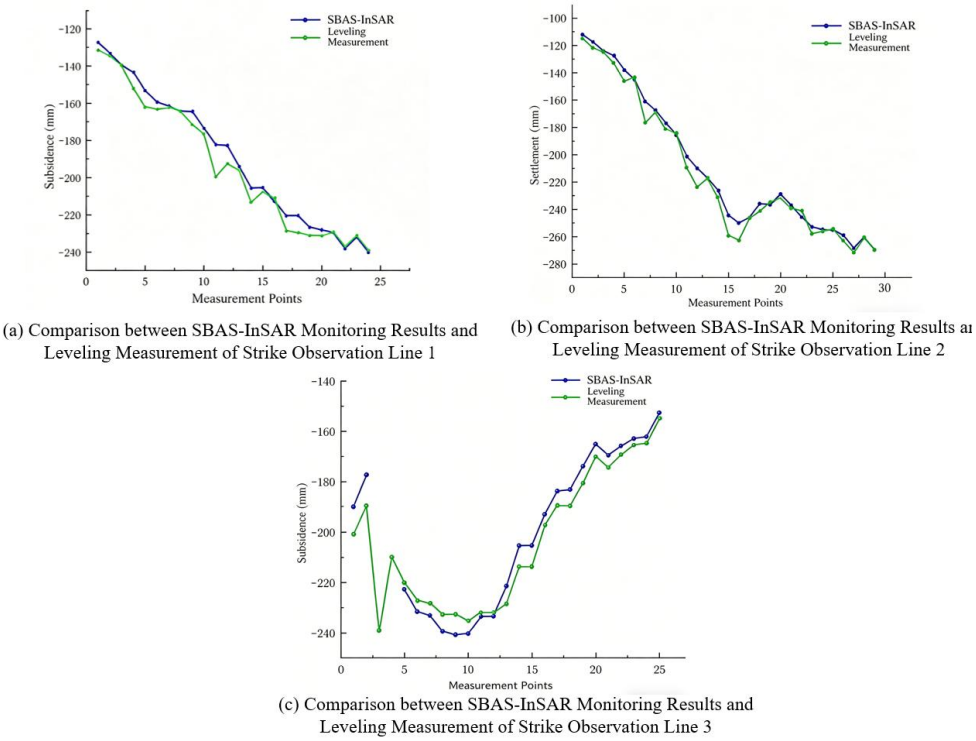
To verify the SBAS-InSAR results, three strike observation lines and two dip observation lines were surveyed by leveling. Comparison graphs are shown in Figures 3 and 4 . Quantitative accuracy indicators are summarized in Table 3.



(a) Inclination Observation Line 1 SBAS-InSAR Monitoring Results and Leveling Measurement Comparison Chart

(b) Inclination Observation Line 2 SBAS-InSAR Monitoring Results and Leveling Measurement Comparison Chart

Figure 3. Comparison of SBAS-InSAR and Leveling Results along Strike Observation Line



(a) Comparison between SBAS-InSAR Monitoring Results and Leveling Measurement of Strike Observation Line 1

(b) Comparison between SBAS-InSAR Monitoring Results ai Leveling Measurement of Strike Observation Line 2

(c) Comparison between SBAS-InSAR Monitoring Results and Leveling Measurement of Strike Observation Line 3

Figure 4. SBAS-InSAR vs Leveling Results on Dip Observation Line

Table 3. Statistical results of InSAR monitoring accuracy for each observation line

Observation line	RMSE (mm)	MAE (mm)	MaxAE (mm)	MinAE (mm)	R^2
Strike line 1	5.9329	4.2792	17.2000	0.1000	0.9711
Strike line 2	6.4153	4.6852	15.2000	0.4000	0.9842
Strike line 3	6.1166	5.4304	12.2000	1.6000	0.9468
Dip line 1	10.610	8.0654	26.1000	0.3000	0.8481
Dip line 2	8.2586	6.0776	19.9000	0.3000	0.9351

The key results are as follows:

- For strike lines, $R^2 \geq 0.9468$, RMSE ≤ 6.42 mm.
- For dip lines, $R^2 = 0.8481$ and 0.9351, RMSE ≤ 10.61 mm.
- For all 117 sample points, the overall $R^2 = 0.958$.
- The maximum absolute error is 26.1 mm, and most errors are within 10 mm.

These statistics confirm that SBAS-InSAR can accurately capture the spatial

distribution and temporal evolution of surface subsidence in a mining area under thick unconsolidated strata and fault influence, meeting engineering requirements for goaf stability evaluation.

5. Conclusion

Based on the SBAS-InSAR time-series monitoring of surface deformation over the 2015–2024 period on the old goaf under thick unconsolidated strata in the Hebi mining area, combined with staged cumulative subsidence analysis, strike/dip profile comparisons, typical point time-series extraction, and accuracy validation against leveling measurements, the following main conclusions are drawn:

(1) The surface subsidence in the study area has experienced a complete four-stage evolution: local occurrence near working faces, gradual expansion and basin formation, multi-panel subsidence superposition, and finally late-stage attenuation. The thick unconsolidated layer (235–250 m) significantly prolongs the residual deformation period.

(2) Faults play a notable control role in the spatial distribution of subsidence. Fault 1 (adjacent to Panels 2301 and 2302) acts as a transitional regulator, causing moderate spatial heterogeneity. Fault 2 (between Panels 2302 and 2303) exhibits a much stronger control, characterized by obvious asymmetric subsidence and distinct hanging-wall/footwall differences, making it the key structural boundary governing differential settlement in the study area.

(3) Accuracy validation against leveling measurements on three strike lines and two dip lines shows that the SBAS-InSAR results are highly consistent with field data (overall R^2 = 0.958, RMSE < 11 mm for dip lines and < 7 mm for strike lines). The technique reliably captures the spatial distribution and temporal evolution of surface subsidence under thick unconsolidated strata and fault influence, meeting engineering requirements for goaf stability evaluation and providing a scientific basis for land reuse and hazard prevention in old mining areas.

References

[1] Massonnet, D. and Feigl, K.L. (1998) Radar Interferometry and Its Application to Changes in the Earth's Surface. Reviews of Geophysics, 36, 441-500.

[2] Rosen, P.A., Hensley, S., Joughin, I.R., Li, F.K., Madsen, S.N., Rodriguez, E. and Goldstein, R.M. (2000) Synthetic Aperture Radar Interferometry. Proceedings of the IEEE, 88, 333-382.

[3] Ferretti, A., Prati, C. and Rocca, F. (2001) Permanent Scatterers in SAR Interferometry. IEEE Transactions on Geoscience and Remote Sensing, 39, 8-20.

[4] Berardino, P., Fornaro, G., Lanari, R. and Sansosti, E. (2002) A New Algorithm for Surface Deformation Monitoring Based on Small Baseline Differential SAR Interferograms. IEEE Transactions on Geoscience and Remote Sensing, 40, 2375-2383.

[5] Hooper, A., Zebker, H., Segall, P. and Kampes, B. (2004) A New Method for Measuring Deformation on Volcanoes and Other Natural Terrains Using InSAR Persistent Scatterers. Geophysical Research Letters, 31, L23611.

[6] Bamler, R. and Hartl, P. (1998) Synthetic Aperture Radar Interferometry. Inverse

Problems, 14, R1-R54.

[7] Li, S., Xu, W. and Li, Z. (2022) Review of the SBAS InSAR Time-Series Algorithms, Applications, and Challenges. Geodesy and Geodynamics, 13, 114-126.

[8] Milczarek, W. (2019) Application of a Small Baseline Subset Time Series Method with Atmospheric Correction in Monitoring Results of Mining Activity on Ground Surface and in Detecting Induced Seismic Events. Remote Sensing, 11, 1008.